Reports

Chaotic Motion of Europa and Ganymede and the Ganymede-Callisto Dichotomy

William C. Tittemore

Europa and Ganymede may have undergone an episode of chaotic motion before the establishment of the current Laplace resonance involving the three inner Galilean satellites. During this episode, the orbital eccentricities of both satellites may have increased dramatically. As a result, the mechanical stresses due to tidal deformation of the satellites' icy lithospheres may have been large enough to result in extensive fracturing, and tidal heating may have melted water ice in the mantles of both satellites, triggering the geological activity that has modified their surfaces since the heavy cratering period. The tidal effects on Ganymede during this episode provide an explanation of the dichotomy between it and Callisto, which have similar bulk properties but very different geological histories.

The Voyager 1 and 2 flybys of the Galilean satellites revealed four dramatically different worlds (*1, 2*). The innermost of these satellites, Io, is currently volcanically active. Europa also has an extremely young surface; geological activity has fractured the ice crust and erased most of the topography of this satellite. Ganymede has a mixture of surface types: relatively dark, heavily cratered "dirty ice" terrain at least 3.8 billion years old (*3*), lighter, less cratered, and significantly modified "grooved" terrain between approximately 3.1 and 3.8 billion years old (*3*), and bright smooth terrain overlying older terrains. In contrast, Callisto, which has bulk properties quite similar to those of Ganymede (Table 1), has a dark, ancient, heavily cratered dirty ice surface.

Intense tidal heating drives the volcanism on Io (*4*)—Jupiter's powerful tides bend and flex the interior of Io as it moves in an eccentric orbit forced by the Laplace resonance involving Io, Europa, and Ganymede (*5*); this bending results in frictional dissipation of energy. Although tidal heating of Europa, augmented by radiogenic heating in the silicate core, may be sufficient to maintain a liquid water layer under the ice crust and drive current resurfacing (*6–8*), more intense heating in the past would have been necessary to melt an initially frozen mantle. Tidal heating of Ganymede in the Laplace resonance is negligible (*9*).

The similar sizes, masses, and densities of Ganymede and Callisto imply that they might have similar geological histories, but this notion is contradicted by the Voyager observations. Superficially, the dark cratered terrain on Ganymede resembles the surface of Callisto, but the younger, brighter grooved and smooth terrains have no Callisto analogs. Some form of geological activity occurred on Ganymede only, or was delayed on Ganymede after the end of the heavy bombardment period. Possible mechanisms for the production of the modified terrains on Ganymede include extensional stress due to global expansion (*10, 11*), diapirism (*12, 13*), liquid-water volcanism (*3*), solid-state ice volcanism (*13*), fracturing above convective upwellings (*11, 12*), and fracturing due to tidal deformation (*12*). Although a number of global properties tend to favor development of geological activity on Ganymede but not Callisto, including Ganymede's larger mass, larger silicate fraction, and its involvement in the Laplace resonance, most evolutionary models predict that similar activity should have occurred on Callisto as well, and therefore special initial conditions are required to explain the Ganymede-Callisto dichotomy. I show in this report that melting and fracturing during a period of chaotic orbital motion may account for the resurfacing of Europa and Ganymede and provide an explanation of the Ganymede-Callisto dichotomy.

Io and Europa have probably undergone significant tidal orbital expansion since their formation (*14*). Differential tidal expansion of satellite orbits may cause them to pass through mean motion commensurabilities (*15*). If the Io-Europa 2:1 resonance is old, Europa and Ganymede may have passed through a 3:1 mean motion commensurability early in the history of the solar system (*14, 16–18*). At this commensurability, the orbital period of Ganymede was approximately three times the orbital period of Europa, so the angular combination $3l_G - l_E$ varied slowly, where l is the mean longitude. The gravitational attraction between the two satellites is strongest near conjunctions. At a mean motion commensurability, the configuration of the satellites is nearly the same at successive conjunctions, and the cumulative effects may lead to significant perturbations of their orbits. The nature of the perturbations depends on how successive conjunctions evolve in a coordinate frame referred to the orbits of one or both satellites, the orbits of which precess because of planetary oblateness. At the 3:1 mean motion commensurability, the most important resonances affecting the orbital eccentricities involve the following three angular combinations:

$$\begin{aligned} &3l_G - l_E - 2\varpi_E \\ &3l_G - l_E - \varpi_E - \varpi_G \qquad (1) \\ &3l_G - l_E - 2\varpi_G \end{aligned}$$

where ϖ is the longitude of pericenter. These angles may either circulate or oscillate, and in the absence of other perturbations, each may be described by a pendulum-like Hamiltonian system [see, for example (*19*)]. The orbital pericenters precess at the rate:

$$\dot{\varpi} \equiv \frac{d\varpi}{dt} \approx \frac{3}{2} n J_2 \left(\frac{R_p}{a}\right)^2 \qquad (2)$$

where n and a are, respectively, the mean angular rate of orbital motion and the orbital semimajor axis, R_p is the equatorial radius of the planet (J, Jupiter), and J_2 is a zonal gravity coefficient parameterizing the planetary oblateness. Because the rate of orbital precession is strongly dependent on the distance from the planet, the frequencies of the above 3:1 resonant terms differ by the "splitting frequency" of approximately $\dot{\varpi}_E - \dot{\varpi}_G$. If this splitting frequency is sufficiently large, the perturbative effects of one resonant term may dominate the effects of the others, and the motion may be described analytically. However, if the splitting frequency is small, the resonant terms may interact strongly.

Because Uranus has a small oblateness [$J_2 = 0.0033$ (*20*)], and the relative masses of the Uranian satellites are large, the splitting frequency is sufficiently small that resonances at past mean-motion commensurabilities among the Uranian satellites interact strongly; such strong interactions result in chaotic behavior (*17, 18, 21–24*), and make

Department of Planetary Sciences, Lunar and Planetary Laboratory, University of Arizona, Tucson, AZ 85721.

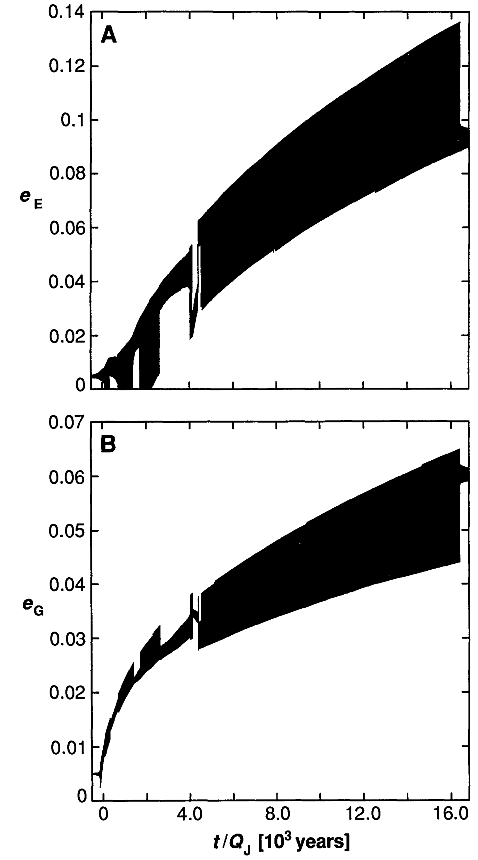

Fig. 1. Orbital eccentricity variations of Europa (**A**) and Ganymede (**B**) during evolution through the 3:1 mean motion commensurability, shown as a function of time referred to the center of the resonance region. The simulated tidal evolution rate corresponds to $Q_J = 2 \times 10^5$ (see text). The dynamical periods are much shorter than the resonance passage time scale, so the shaded region shows the maximum and minimum excursions of eccentricity, calculated at intervals of $t/Q_J = 2.5$ years. Escape from the resonance occurs at $t/Q_J = 1.64 \times 10^4$ years.

capture into some of the resonances only temporary phenomena. Passage through these chaotic resonances can account for Miranda's anomalously large orbital inclination (*17*) and may have resulted in significant tidal heating of Miranda (*22, 24*) and Ariel (*18*). Jupiter has a significantly larger mass, radius, and oblateness [$J_2 = 0.0147$ (*20*)] than Uranus, which favor larger orbital precession rates, and therefore large splitting frequencies. However, the relatively large orbital distances of Europa and Ganymede result in orbital precession rates, and therefore splitting frequencies, that are comparable to those of the inner Uranian satellites. In addition, the relative masses of the Galilean satellites are comparable to those of the Uranian satellites, and thus the resonances should be comparable strength. These factors suggest that chaotic behavior may have been important in the Jovian satellite system.

I have therefore investigated the past dynamical behavior of Europa and Ganymede during evolution through the 3:1 mean motion commensurability, using numerical and analytical techniques similar to those applied to the Uranian satellites (*17, 18, 21–24*). The tidally evolving resonant system is approximated by a truncated, averaged Hamiltonian with a slowly evolving parameter, and algebraic mappings are used for the numerical integrations; selective verification of dynamical behavior is made with standard integration methods. I have restricted my study to the planar two-satellite approximation (*25*), which contains enough of the important dynamical features of the problem to evaluate the possible importance of chaotic behavior at this resonance.

In this approximation, the orbital eccentricities of Europa and Ganymede may increase dramatically during evolution through the 3:1 commensurability (Fig. 1). A total of 29 trajectories were evolved through the Europa-Ganymede 3:1 resonance, and the simulated tidal evolution rates correspond to $Q_J = 2 \times 10^5$, 8×10^3, and 2×10^3 [for $k_{2J} = 0.379$ (*26, 27*)]. In all cases, the maximum orbital eccentricities before the satellites escape from the resonance are much larger than the current values (Fig. 2 and Table 1), and the distributions of maximum eccentricity are similar for the different rates (*28*). Eccentricities upon escape from the resonance are lower than the maximum eccentricities by approximately 0.005 for Ganymede and 0.02 to 0.04 for Europa. Two trajectories (not included in Fig. 2) did not enter the large chaotic zone and were captured into resonance.

In the planar two-satellite approximation, the dynamical equations of motion can be approximated by a Hamiltonian system with two degrees of freedom. For such a system, it is possible to portray the phase space in two dimensions with the surface of section or Poincare map [see (*29*)]. The generalized coordinates of the planar-eccentric 3:1 resonance Hamiltonian are related to two of the resonance angles defined above:

$$\sigma_E = \frac{1}{2}(3l_G - l_E - 2\varpi_E)$$

$$\sigma_G = \frac{1}{2}(3l_G - l_E - 2\varpi_G) \qquad (3)$$

and the momenta are proportional to e_E^2 and e_G^2, respectively [see, for example, (*22*)]. The surface of section is made by plotting e_G versus σ_G when $\sigma_E = 0$. Points generated by chaotic trajectories fill areas on the phase plane in an irregular manner; quasiperiodic trajectories generate points that lie on curves.

Table 1. Satellite parameters. Parameter values are taken from Burns (*20*).

Satellite	Density ($g\ cm^{-3}$)	Mass (10^{25} g)	Radius (10^8 cm)	Semimajor axis (10^{10} cm)	Eccentricity (forced) free	Inclination (degrees)
Europa	2.97	4.80	1.569	6.709	(0.0101) 10^{-4}	0.470
Ganymede	1.94	14.823	2.631	10.70	(0.0006) 0.0015	0.195
Callisto	1.86	10.766	2.400	18.83	0.007	0.281

Soon after encountering the 3:1 resonance the trajectory in Fig. 1 enters a chaotic zone (Fig. 3), which dominates the phase space until escape from the resonance. The trajectory crosses between the chaotic zone and the quasiperiodic resonance zones; this results in the very ragged appearance in Fig. 1 before $t/Q_J \simeq 4.5 \times 10^3$. After this point, the chaotic zone fills nearly all of the resonance region; the maximum and minimum excursions of eccentricity vary smoothly for the most part, although the variations within these bounds are typically chaotic (*30*).

The presence of a chaotic zone leading to large orbital eccentricities at the 3:1 resonance strongly suggests that it played an important role in the thermal evolution of Europa and Ganymede. If the satellites reached eccentricities of the order of those shown in Fig. 2 during passage through the 3:1 resonance, tidal distortion of the satellites may have had important geophysical consequences. A synchronously rotating satellite in an eccentric orbit is tidally heated at a rate (*31*)

$$\frac{dE}{dt} \approx \frac{63}{38}\frac{m_p n^3 \rho g R^6}{\mu a^3 Q_s} e^2 \qquad (4)$$

where m_p is the mass of the planet, and ρ, g, R, μ, and Q_s are, respectively, the density, surface gravity, radius, rigidity, and specific dissipation function (*27*) of the satellite. In addition, the satellites are radiogenically heated; the primordial equilibrium radiogenic heat fluxes of Europa and Ganymede were approximately 65 erg s^{-1} cm^{-2} and 40 erg s^{-1} cm^{-2}, respectively, and would have decayed to approximately 60% of these values after a billion years (*9*).

Reynolds and Cassen (*32*) calculated that solid-state convection in the mantles of large, differentiated icy satellites could remove an equilibrium heat flux of up to 115 erg s^{-1} cm^{-2}. By combining the above two heat sources, we may estimate the critical orbital eccentricities necessary to overcome

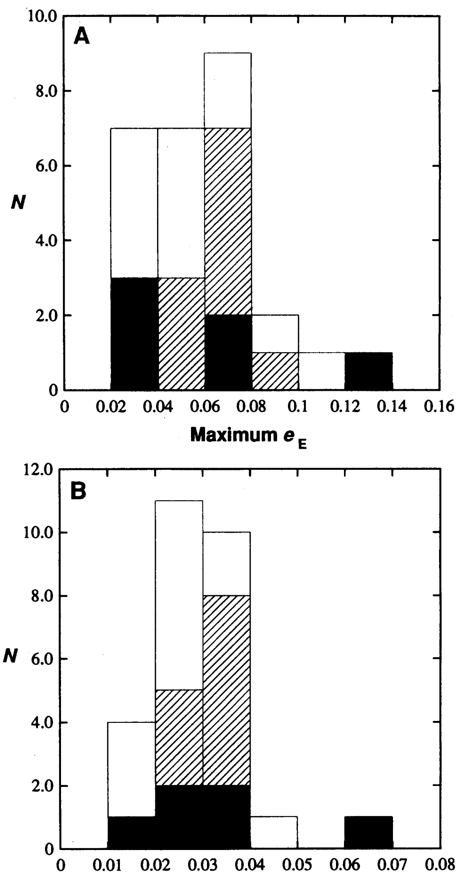

Fig. 2. Maximum eccentricities of Europa (**A**) and Ganymede (**B**) before escaping from the 3:1 mean motion commensurability. Black, effective $Q_J = 2 \times 10^5$; hatched, effective $Q_J = 8 \times 10^3$; white, effective $Q_J = 2 \times 10^3$.

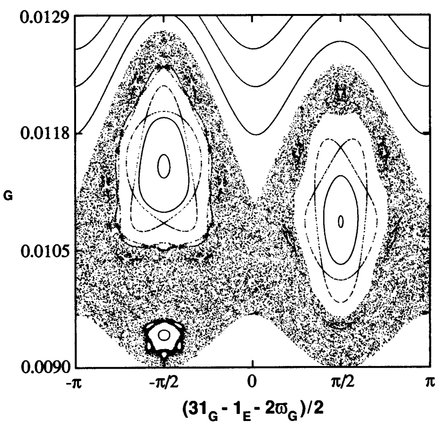

Fig. 3. Surface of section for the trajectory in Fig. 1 at $t/Q_J = 1.56 \times 10^2$, shortly after the trajectory has entered the chaotic zone. The quasiperiodic regions above and below the chaotic zone are regions away from the resonance where σ_G circulates. The two large quasiperiodic regions engulfed by the chaotic zone are regions where σ_G librates, and the small quasiperiodic zone amid the chaotic zone at lower right is the region where the resonance angle $3l_G - l_E - \varpi_E - \varpi_G$ librates. Here, the resonances overlap, that is, the chaotic separatrices have merged. The chains of islands visible in the libration regions are the chaotic separatrices associated with secondary resonances between the libration frequency and the splitting frequency. These secondary resonances transfer trajectories from the quasiperiodic libration regions into the chaotic zone [see, for example (*17, 18, 22*)]. At larger values of the eccentricity, the resonant libration regions shrink, and the chaotic zone occupies most of the resonance region. The eccentricity scale is nonlinear on this plot.

solid-state convection in the satellites' interiors and to lead to the melting of water ice, assuming that Europa and Ganymede were solid and differentiated approaching the resonance and that they were in thermal equilibrium with the heat sources.

For these calculations, I used rigidities of 6.5×10^{11} dyne cm^{-2} for Europa and 4×10^{10} dyne cm^{-2} for Ganymede [following (*9*)]. A billion years after the satellites formed, during the phase of geological activity leading to the production of the grooved terrain on Ganymede (*3*), the critical eccentricities for Europa and Ganymede would have been:

$$e_{E_{cr}} = 0.0020\, Q_E^{1/2}$$
$$e_{G_{cr}} = 0.0039\, Q_G^{1/2} \qquad (5)$$

Tidal Q's of satellites may be as low as 10 if the interior is near the solidus temperature, or as large as 500 if cold [see, for example (*33*)]. For values of Q_E within this range, and for Q_G less than about 200, many of the maximum eccentricities summarized in Fig. 2 are comparable to or exceed the above critical values, and thus melting of water ice in the mantles of these satellites may have been possible during passage through the 3:1 resonance.

Whether melting actually occurred depends on both the magnitude and duration of tidal heating. The maximum orbital eccentricities attainable by the satellites are constrained by the rates of tidal dissipation in the planet and the satellites [see, for example (*22*)]. The larger the dissipation rate in Jupiter, the more rapid the expansion of Europa's orbit, and therefore, the larger the possible maximum eccentricities. The much more rapid orbital expansion of Io sets an upper limit on the rate of tidal evolution required if Europa and Ganymede were to evolve through the 3:1 resonance before the establishment of the Io-Europa 2:1 resonance. This upper limit is about an order of magnitude too small to allow the critical melting eccentricities (*34–36*). However, if the Io-Europa 2:1 resonance was established before the Europa-Ganymede 3:1 resonance was encountered, tidal torques on Io would have increased the rate of Europa's orbital expansion and its approach to the resonance by about a factor of 20 (*5, 14*). Therefore, for significant heating of Europa and Ganymede to have occurred, the Io-Europa 2:1 resonance must have been established before Europa and Ganymede escaped from the 3:1 resonance.

At such a rapid tidal evolution rate, the time scale for resonance passage would have been only a few times 10^5 years or less. Most of the tidal heating of Ganymede probably occurred after escape from the resonance as its orbital eccentricity decreased exponentially with a time decay constant $\tau \approx 10^6\, Q_G$ years. The internal temperature of Ganymede at the time of resonance encounter was probably at least 220 K, a value that even may have been reached by much smaller icy satellites of Saturn as a result of accretional and radiogenic heating only (*37*). The minimum melting temperature of water ice in the interior of Ganymede is approximately 253 K (*32*), so that in order for melting to have occurred, the internal temperature of Ganymede must have increased by up to $\Delta T \approx 33$ K while the rate of tidal heating still exceeded the maximum rate of convective heat loss. The interval of time during which e_G remained above the critical value is at most a few times 10^7 years for $10 < Q_G < 200$; heat is distributed within Ganymede by solid-state convection on a similar time scale, on the basis of estimates of the convective velocities of order 10 to 100 cm yr^{-1} in the ice mantle (*11*). In the approximation that all of the heat tidally generated during this interval was retained, the escape eccentricity required for the melting of water ice is [see also (*18*)]

$$e_{G_{esc}} = \left(\frac{2\Delta T a_G C}{G m_p} + e_{G_{cr}}^2 \right)^{1/2} \qquad (6)$$

where G is the gravitational constant and $C \approx 2 \times 10^7$ erg g^{-1} K^{-1} is the heat capacity. For $\Delta T = 33$ K, this equation yields $0.035 < e_{G_{esc}} < 0.064$ for $10 < Q_G < 200$, values that may have been reached by Ganymede during evolution through the 3:1 resonance (Fig. 2). The greatest uncertainty in this scenario is the effect of Io on the dynamics of resonance passage (*38*). Further work is warranted to better determine the probability that melting occurred.

Even if the orbital eccentricity of Ganymede did not reach the values given above, tidal heating at the 3:1 resonance may have significantly affected its thermal evolution. For example, if Ganymede was undifferentiated at the time of resonance encounter, the presence of silicates in the mantle ice may have reduced the efficiency of solid-state convection (*39, 40*), and melting of water ice may have occurred even if the maximum eccentricities were smaller than the critical values given above. Also, if significant amounts of materials with much lower melting temperatures, such as the ammonia water eutectic, were present, mobilization of mantle material may have occurred at eccentricities smaller than those required to melt water ice.

In addition to the possibility of melting, tidal deformation of the satellites during resonance passage may have stressed the rigid lithospheres of Europa and Ganymede sufficiently to cause widespread fracturing, which would have provided conduits through which mobile mantle material could resurface. The periodic variations in the tidal distortion of a satellite in an eccentric orbit give rise to stress on the lithosphere; the magnitude of the stress is proportional to e/a^3 (*12, 41, 42*). Because the Maxwell time of Europa's lithosphere is of the order of an orbital period (*8*) and that of Ganymede's lithosphere is much longer than an orbital period (*13*), a nearly elastic response of the lithospheres to tidal stresses is expected, and brittle failure may occur if the stress is sufficiently large. Currently, tidal stresses are of the order of a few bars on both satellites, more than an order of magnitude too small to cause fracturing (*7, 12, 43*). At the 3:1 resonance, tidal stresses on the lithospheres of Europa and Ganymede would have been enhanced over the current values by factors of approximately $2 \times 10^2 e_E$ and $7 \times 10^2 e_G$, respectively. At the largest values of eccentricity attained by the satellites for the trajectory in Fig. 1, tidal stresses would have been enhanced by about a factor of 30 for Europa and a factor of 50 for Ganymede, and may have caused extensive fracturing.

The possibility of a significant heat source at the 3:1 commensurability is consistent with some other models for the resurfacing of Ganymede. If Ganymede and Callisto were both deeply differentiated during accretion, freezing of the ice mantle from above and below may have culminated in a convective instability as solid-state convection bridged the residual liquid water layer (*13*). Diapiric transfer of heat from the interior may have occurred, and this process may have resulted in fracturing of the brittle upper lithosphere and the emplacement of relatively warm, clean ice on the surface. If this occurred during the heavy cratering period, the geological evidence would have been obliterated by impacts. However, if tidal heating led to the melting and fracturing of the ice mantle of Ganymede during passage through the 3:1 resonance after heavy bombardment, a second instability may also have occurred in Ganymede only as the mantle froze again after resonance passage; such an event could result in a second phase of surface activity.

Alternatively, if Ganymede and Callisto were both only partly differentiated during accretion, both may have possessed an "accretional trigger" (*40*), that is, the interface between an icy differentiated upper mantle and an undifferentiated lower mantle may have been a barrier to solid-state convection, making the melting of water ice more likely in the ice-rock lower mantle than in a fully differentiated ice mantle. If melting were initiated below the interface between the upper and lower mantles, a runaway differentiation (*39*) might be triggered. Perhaps only Ganymede was heated sufficiently during passage through the 3:1 resonance to pull the trigger and initiate runaway differentiation, while Callisto remained only partly differentiated. During runaway differentiation, further melting of the ice and global expansion of Ganymede (*10*) may have occurred, and as the now differentiated mantle froze, it may have become susceptible to the convective instability of Kirk and Stevenson (*13*), which would result in yet more modification of the surface. Either way, a combination of melting and fracturing due to tidal effects and the resurfacing mechanisms described above may account for the timing and duration of the resurfacing of Ganymede following the heavy cratering period.

REFERENCES AND NOTES

1. B. A. Smith *et al.*, *Science* **204**, 951 (1979).
2. ——— *et al.*, *ibid.* **206**, 927 (1979).
3. E. M. Shoemaker, B. K. Lucchitta, J. B. Plescia, S. W. Squyres, D. E. Wilhelms, in *Satellites of Jupiter*, D. Morrison, Ed. (Univ. of Arizona Press, Tucson, 1982), pp. 435–520.
4. S. J. Peale, P. Cassen, R. T. Reynolds, *Science* **203**, 892 (1979).
5. C. F. Yoder, *Nature* **279**, 767 (1979).
6. S. W. Squyres, R. T. Reynolds, P. M. Cassen, S. J. Peale, *ibid.* **301**, 225 (1983).
7. M. N. Ross and G. Schubert, *ibid.* **325**, 133 (1987).
8. G. W. Ojakangas and D. J. Stevenson, *Icarus* **81**, 220 (1989).
9. P. M. Cassen, S. J. Peale, R. T. Reynolds, in *Satellites of Jupiter*, D. Morrison, Ed. (Univ. of Arizona Press, Tucson, 1982), pp. 93–128.
10. S. W. Squyres, *Geophys. Res. Lett.* **7**, 593 (1980).
11. ——— and S. K. Croft, in *Satellites*, J. Burns and M. S. Matthews, Eds. (Univ. of Arizona Press, Tucson, 1986), pp. 293–341.
12. E. M. Parmentier and J. W. Head, *J. Geophys. Res.* **84**, 6263 (1979).
13. R. L. Kirk and D. J. Stevenson, *Icarus* **69**, 91 (1987).
14. C. F. Yoder and S. J. Peale, *ibid.* **47**, 1 (1981).
15. P. Goldreich, *Mon. Not. Roy. Astron. Soc.* **130**, 159 (1965).
16. Yoder and Peale (*14*) concluded that Europa and Ganymede probably did not evolve through the 3:1 resonance, on the basis of an analytically derived capture probability of about 80% into any one of the three important second-order inclination resonances associated with the Europa-Ganymede 3:1 commensurability. However, application of the perturbed resonance model (*17, 18*) indicates that chaotic behavior may be important at these inclination resonances, so I numerically determined the probability of escape from the inclination resonances using the dynamical model in (*17*). Preresonance values of the inclinations ($i_E = 0.8541°$ and $i_G = 0.3063°$) were obtained by integrating a trajectory with the current inclinations (Table 1) backwards in time through the 3:1 inclination resonances. A total of 100 trajectories that are dynamically equivalent except for the angular phases were calculated from this initial set of coordinates and were numerically evolved through the inclination resonances at a simulated tidal evolution rate corresponding to $Q_J = 2 \times 10^3$. Of the 100 trajectories, 49 escaped from the resonances altogether. A more limited numerical set of ten trajectories was evolved through the inclination resonances at a rate 1/10 as fast, and of these, six escaped from the inclination resonances altogether. The mean values and standard deviations of the time-averaged orbital inclinations after resonance passage are: for $Q_J = 2 \times 10^3$, $\langle i_E \rangle = 0.4637° \pm 0.0005°$ and $\langle i_G \rangle = 0.2128° \pm 0.0056°$, and for $Q_J = 2 \times 10^4$, $\langle i_E \rangle = 0.4493° \pm 0.0006°$ and $\langle i_G \rangle = 0.2113° \pm 0.0186°$, in both cases near the current values. Both numerical experiments yielded a significantly larger probability of escape than calculated by Yoder and Peale (*14*).
17. W. C. Tittemore and J. Wisdom, *Icarus* **78**, 63 (1989).
18. W. C. Tittemore, *ibid.*, in press.
19. S. J. Peale, *Annu. Rev. Astron. Astrophys.* **14**, 215 (1974).
20. J. A. Burns, in *Satellites*, J. Burns and M. S. Matthews, Eds. (Univ. of Arizona Press, Tucson, 1986), pp. 1–38.
21. W. C. Tittemore and J. Wisdom, *Icarus* **74**, 172 (1988).
22. ———, *ibid.* **85**, 394 (1990).
23. S. F. Dermott, R. Malhotra, C. D. Murray, *ibid.* **76**, 295 (1988).
24. R. Malhotra and S. F. Dermott, *ibid.* **85**, 444 (1990).
25. Numerical values of the Hamiltonian coefficients were evaluated at $a_E = 7.2114 R_J$ and $a_G = 14.99 R_J$. At the Europa-Ganymede 3:1 mean motion commensurability, the semimajor axis ratio (a_E/a_G) increases with time, because of the more rapid orbital expansion of Europa. For the numerical integrations, $e_E = e_G = 0.005$ before resonance encounter.
26. S. V. Gavrilov and V. N. Zharkov, *Icarus* **32**, 443 (1977).
27. The specific dissipation function Q is defined by

$$Q = 2\pi \frac{E_p}{\oint (dE/dt)dt} \tag{7}$$

where E_p is the peak energy stored in a tidal cycle, and $\oint (dE/dt)dt$ is the energy dissipated over a complete tidal cycle. A satellite's orbital expansion rate is inversely proportional to the tidal Q of the planet; k_2 is the second-order Love number.
28. Tittemore and Wisdom (*17, 21, 22*) found that because of the great difference between the dynamical and tidal timescales, the dynamics of chaotic resonance passage may be independent of the simulated tidal rate if the rate is below a chaotic adiabatic value, which is typically orders of magnitude larger than rates corresponding to physical values of Q. Therefore, the dynamical behavior displayed in Fig. 1 represents what the actual behavior may have been, independent of our uncertainty about the actual value of Q_J during resonance passage.
29. M. Hénon and C. Heiles, *Astron. J.* **69**, 73 (1964).
30. The numerical experiments do not include dissipation in the satellites, which may affect the dynamics at large eccentricities. However, the chaotic variations of eccentricity are on a much shorter time scale than the tidal time scale. Dissipation in the satellites likely controls the maximum average eccentricities reached by the satellites before escape, but probably does not affect the extent of the relatively rapid chaotic variations.
31. S. J. Peale and P. Cassen, *Icarus* **36**, 245 (1978).
32. R. T. Reynolds and P. M. Cassen, *Geophys. Res. Lett.* **6**, 121 (1979).
33. S. J. Peale, P. Cassen, R. T. Reynolds, *Icarus* **43**, 65 (1980).
34. The maximum resonance passage time scale, if Europa and Ganymede entered the 3:1 resonance right after formation, is the time it takes for Io to evolve from synchronous orbit until $n_I = 2n_E$, where $n_E = 3n_G$ [see, for example (*35*)]. For Io to remain away from the Io-Europa 2:1 resonance up to 3.8 billion years ago (the age of the oldest modified terrains on Ganymede) or more recently,

$Q_J > 2.8 \times 10^5$. In an orbital resonance, the amount of energy available to heat the satellites by tidal dissipation is the difference between the rate at which work is done on the satellites by tidal torques and the rate at which the orbital energies increase [see, for example (*36*)]. By equating this difference to the sum of the minimal melting heating rates of Europa and Ganymede, I estimate that a maximum Q_J of 1.4×10^4 or less is required for both satellites to reach the critical melting eccentricities during passage through the 3:1 resonance, if the Io-Europa 2:1 resonance was not yet established.
35. P. Goldreich and S. Soter, *Icarus* **5**, 375 (1966).
36. S. J. Peale, *ibid.* **74**, 153 (1988).
37. K. Ellsworth and G. Schubert, *Icarus* **54**, 490 (1983).
38. It is possible that the Io-Europa 2:1 resonance remained stable during evolution through the weaker Europa-Ganymede 3:1 resonance, despite the presence of a chaotic zone. I have carried out some numerical integrations of Io and Europa through the 2:1 resonance, and the results indicate that for small initial eccentricities, capture into this resonance is very likely. Tittemore and Wisdom (*22*) showed that Ariel and Umbriel, which exhibit similar behavior at the 2:1 resonance, may remain captured in the resonance even if on a chaotic trajectory. Interference from Io would not likely change the chaotic 3:1 resonance behavior to quasi-periodic behavior.
39. A. J. Friedson and D. J. Stevenson, *Icarus* **56**, 1 (1983).
40. S. Mueller and W. B. McKinnon, *ibid.* **76**, 437 (1988).
41. P. Helfenstein and E. M. Parmentier, *ibid.* **53**, 415 (1983).
42. ———, *ibid.* **61**, 175 (1985).
43. G. D. Crawford and D. J. Stevenson, *ibid.* **73**, 66 (1988).
44. This research was supported in part by the NASA Planetary Geology and Geophysics Program under grant NAGW-1720. This paper is contribution #90-29 of the University of Arizona Theoretical Astrophysics Program.

16 April 1990; accepted 6 August 1990

A Plant Leucine Zipper Protein That Recognizes an Abscisic Acid Response Element

MARK J. GUILTINAN, WILLIAM R. MARCOTTE, JR., RALPH S. QUATRANO*

The mechanism by which phytohormones, like abscisic acid (ABA), regulate gene expression is unknown. An activity in nuclear extracts that interacts with the ABA response element (ABRE) from the 5' regulatory region of the wheat *Em* gene was identified. A complementary DNA clone was isolated whose product is a DNA binding protein (EmBP-1) that interacts specifically with an 8–base pair (bp) sequence (CACGTGGC) in the ABRE. A 2-bp mutation in this sequence prevented binding of EmBP-1. The same mutation reduced the ability of the ABRE to confer ABA responsiveness on a viral promoter in a transient assay. The 8-bp EmBP-1 target sequence was found to be conserved in several other ABA-responsive promoters and in promoters from plants that respond to signals other than ABA. Similar sequences are found in promoters from mammals, yeast, and in the major late promoter of adenovirus. The deduced amino acid sequence of EmBP-1 contains conserved basic and leucine zipper domains found in transcription factors in plants, yeast, and mammals. EmBP-1 may be a member of a highly conserved family of proteins that recognize a core sequence found in the regulatory regions of various genes that are integrated into a number of different response pathways.

RESPONSES OF CELLS TO EXTERNAL stimuli (such as light, hormones, and environmental stress) are mediated in part by the expression of genes whose products contribute to a given physiological effect. Studies with animal hormones have elucidated several response pathways that ultimately converge at the level of gene expression (*1, 2*). These pathways have been deciphered in part through identification of the protein factors that bind regulatory elements in hormone-responsive genes. The distinct transcriptional regulatory patterns of genes expressed during these responses are determined primarily by specific interactions between protein and DNA (*1, 2*).

Department of Biology, The University of North Carolina at Chapel Hill, Chapel Hill, NC 27599–3280.

*To whom correspondence should be addressed.

During plant development, hormones influence fruit ripening, seed maturation and germination, shoot and root growth, and responses to environmental and pathogenic stresses (*3*). However, the response pathway for any one phytohormone has not yet been elucidated. All classes of phytohormones influence the expression of specific genes, at least in part at the level of transcription (*4, 5*). Related sequences exist in the 5' upstream regions of genes similarly regulated either by abscisic acid (ABA), gibberellic acid (GA), ethylene, or auxin (*6–8*). DNA regulatory elements have been functionally identified in promoters of genes responsive to ABA (*9–11*), GA (*12*), and ethylene (*7*).

Like most phytohormones, ABA mediates diverse physiological responses, including promotion of embryogenesis and prevention of precocious germination (*5, 13*). Late in seed development of a wide variety of plants, a unique set of abundant mRNAs and proteins appear, coincident with high concentrations of endogenous ABA. These late embryo abundant (Lea) gene products share common physical properties and accumulate in mature embryos (*13, 14*). If embryos are isolated at earlier developmental stages and exposed to exogenous ABA, some of the Lea class mRNAs and proteins accumulate precociously (*5, 13–15*). The concentration of ABA also increases when plant tissues are stressed by desiccation (*16*), wounding (*17*), or high osmoticum (*18*), resulting in the expression of some of the same Lea genes in nonembryonic tissues (*13*). We approached the question of how ABA exerts its effect at the level of the gene by defining regulatory elements in the ABA-responsive promoter of the wheat *Em* gene (*9, 10, 19*).

Accumulation of mRNA from *Em* (*20, 21*) is regulated by ABA during embryo development and under stress conditions (*5, 13, 19*) in a manner similar to other Lea genes. When the *Em* 5' regulatory region was linked to the reporter gene, β-glucuronidase (GUS), and used in transient (*9*) and transgenic (*10*) assays, a 646-bp region (−554 to +92) that was essential for response to ABA was identified. Within this region, a 50-bp ABA response element (ABRE) (−152 to −103) has been defined that is capable of conferring ABA inducibility upon a minimal cauliflower mosaic virus (CaMV) promoter (*10*). Two elements (Em1 and Em2) within this 50-bp ABRE are conserved in other ABA-regulated promoters (*10*), including the rice *Rab* and the cotton Lea gene families (*8, 11*). We now describe the identification of a protein that interacts with the ABRE.

Nuclear extracts from mature wheat embryos and rice cells in suspension cultures contained proteins that bound a ^{32}P-labeled 119-bp DNA fragment (ABRE probe) that contained the 50-bp response element (Fig. 1) (*22*). Two major protein-DNA complexes (B1 and B2) were specifically competed by unlabeled DNA fragments that contained the ABRE (Fig. 1B). Neither the *Em* coding sequence nor an ABRE that contained a 2-bp mutation (mABRE) was capable of competing for the binding activity (Fig. 1B).

We noticed that the recognition site (Hex) for the wheat transcription factor HBP-1 (*23*) contains sequences that are similar to the ABRE (Fig. 1A). A DNA fragment that contained the Hex sequence was capable of competing with the ABRE probe for binding activity (Fig. 1B), but did not compete as well as the ABRE fragment (Fig. 1B).